A Stable Lipid-Induced Aggregate of α-Synuclein

Malte Drescher,[†,§] Bart D. van Rooijen,[‡] Gertjan Veldhuis,[‡,∥] Vinod Subramaniam,*[,‡] and Martina Huber*[,†]

Department of Molecular Physics, Leiden University, P.O. Box 9504, 2300 RA Leiden, The Netherlands, and Nanobiophysics, MESA+ Institute for Nanotechnology & MIRA Institute for Biomedical Technology and Technical Medicine, University of Twente, P.O. Box 217, 7500AE Enschede, The Netherlands

Received November 4, 2009; E-mail: v.subramaniam@tnw.utwente.nl; mhuber@molphys.leidenuniv.nl

α-Synuclein (αS) is a 140 residue protein constituting the major component of Lewy bodies found in Parkinson's disease,[1,2] where it is aggregated into fibrils.[3] Although the exact function of αS is yet to be determined, the interaction of αS with synaptic vesicles has been suggested to be important for its physiological role.[3−5] While αS is natively unfolded in solution,[6] upon binding to negatively charged membranes it adopts an amphipathic, α-helical structure involving residues 1−100.[7−13] Membrane binding is also thought to affect fibrillization, although conflicting evidence exists on whether membrane binding enhances or reduces the propensity of αS to form fibrils.[3,13] Simulations and an experimental observation point to the potential of αS to form aggregates on membranes.[14−19] Experimental information on the structure of such aggregates is lacking, but it has been proposed that specific membrane-associated aggregates could act as seeds for αS fibrils.[14] Here we present evidence for αS aggregates on membranes and present a model for the simplest structure of such an aggregate.

Previously, we have shown that individual αS monomers adopt a horseshoe-type conformation when interacting with negatively charged POPG [1-Palmitoyl-2-Oleoyl-*sn*-Glycero-3-(Phosphorac-(1-glycerol))] small unilamellar vesicles (SUVs).[20] This observation was made by measuring the distance between two spin labels attached to αS (*intra*molecular distance) using a two-frequency, pulsed EPR method (double electron−electron resonance DEER or pulsed electron−electron double resonance PELDOR).[21−25] Here we present DEER measurements on αS labeled with a single spin label to determine *inter*molecular distances. Such *inter*molecular interactions had been carefully excluded in the previous study.[20] Here, we show that αS forms aggregates once in contact with the SUVs. These aggregates have a well-defined structure, which can be modeled with a dimer as the simplest unit. Thus, upon contact with these SUVs, αS forms supramolecular, well-ordered arrays with well-defined molecular contacts.

Furthermore, there are indications that αS may influence the membrane structure or even disrupt membranes causing membrane leakage, a finding that is of potential relevance to the disease related effects of αS.[26] We present evidence that the structure of the POPG SUVs is affected by the presence of αS, consistent with a recent report.[27]

Single-cysteine mutants of αS specifically labeled with MTSL were investigated: αS with a spin label at position 9 (αS9), and
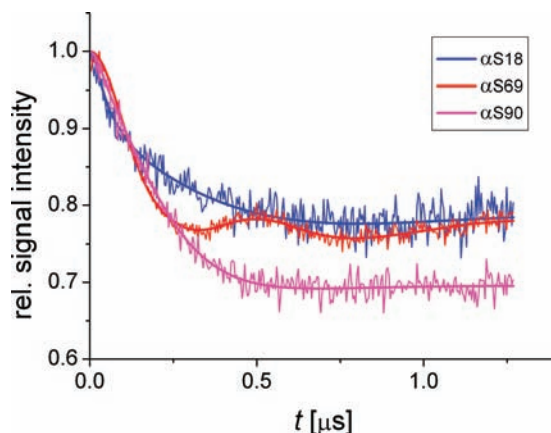

Figure 1. Experimental DEER traces after background correction for singly labeled αS upon addition of negatively charged SUVs (thin lines). The corresponding fit (thick lines) is based on distance distributions depicted in Figure 2 derived by Tikhonov regularization.

αS18, αS69, and αS90. Evidence for aggregation is threefold. Correlated distances, i.e. well-defined distances between pairs of spins giving rise to DEER modulation, are observed for singly labeled αS, showing that the interactions are intermolecular. The distances depend on the position that is labeled, indicating a well-defined, specific structure. Changing the peptide-lipid-ratio from 1/250 to 1/1000 did not affect the distance distributions.

Distances were measured for αS incubated with SUVs and compared to the distances obtained in the absence of vesicles, i.e. for αS free in solution. In the absence of vesicles, the DEER responses of all four mutants are well described by a homogeneous, three-dimensional distribution of spins, as expected for monomeric αS. For αS incubated with vesicles, the DEER time traces of all mutants except αS9 became significantly nonexponential corresponding to distinct intermolecular distance distributions (Figure 1).

Model-free analysis of the DEER time traces[23] yields two clearly distinguishable peaks for all mutants except αS9 (Figure 2).

The number of spins contributing to each distance distribution is close to two for αS18, αS69, and αS90 (see Table 1), revealing that these distances are due to a pair of interacting spins. The peaks are broad (full width at half-maximum >1 nm), reflecting the flexibility of the spin-label linker and the heterogeneity of the arrangement. The observation of two distances suggests two types of αS-dimers, which we term A and B. Distances are listed in Table 1.
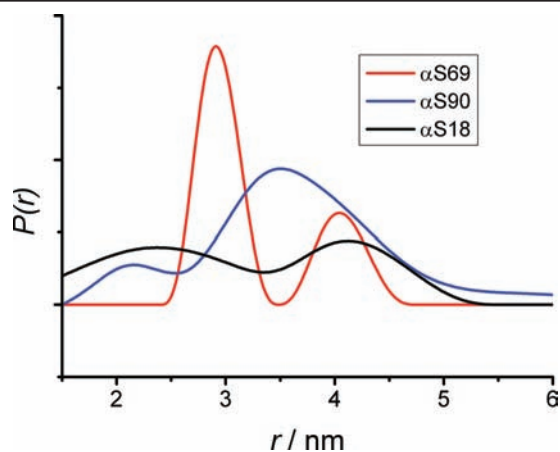
Figure 2. Intermolecular distance distributions derived by Tikhonov regularization from the DEER traces of different singly labeled αS mutants. Arrows indicate extracted distances as listed in Table 1.

Table 1. Comparison between Experimental Intermolecular Distances and Values Predicted by the Proposed Dimer Model (Figure 3) of αS

αS mutant	spins/aggregate[a]	distance model dimer A/nm	distance (DEER)/nm	distance model dimer B/nm	distance (DEER)/nm
αS9	n.a.[b]	4.7	—[c]	1.2	—
αS18	1.8 ± 0.2	4.3	4.2	2.2	2.4
αS69	2.0 ± 0.2	3.0	2.9	4.2	4.0
αS90	2.2 ± 0.2	3.5	3.5	2.3	2.1
αS9/αS69	1.9 ± 0.2	2.3	2.3	4.3, 3.4	4.1
αS9/αS 90	1.6 ± 0.2	2.7	3.0	3.5, 2.3	3.8, 2.3
αS18/αS69	1.7 ± 0.2	2.5	2.1	4.5, 3.7	4.2
αS69/αS90	2.2 ± 0.2	0.9	—	1.2	—

[a] As derived from the modulation depth of the DEER trace. Incomplete labeling was taken into account. For error determination see Supporting Information. [b] Not available; see footnote c. [c] No distinct distances detected within the experimentally accessible range of distances (for details see Supporting Information).

For the case of two different dimers, 1:1 mixtures of different αS mutants (mutant I, αS(I), and mutant II, αS(II)) should yield the sum of the distance distributions of the individual mutants plus additional distances deriving from pairs of αS(I) and αS(II). Distance distributions observed for those mixtures of different αS mutants agree with the predictions from the model (Table 1).

Based on the experimental inter- and intramolecular[20] distances, a model for the coexisting dimer types A and B can be constructed (Figure 3). Models based on the assumption that αS molecules are in an extended helix conformation, as suggested for membrane bound monomeric αS in some studies,[12,28] do not agree with the experimental data presented here. In contrast, a dimer model assuming the horseshoe conformation[13,20,29,30] and colocalization of the α-helical regions of the two αS molecules in a single plane, as depicted in Figure 3, represents a viable interpretation of the distance constraints derived from the experiments.

In both dimers, A and B, the C-terminal ends of helix 2 of both monomer partners are close to each other, in an antiparallel arrangement. While helix 1 is facing outward in dimer A, in dimer B the two N-termini of the individual monomers face each
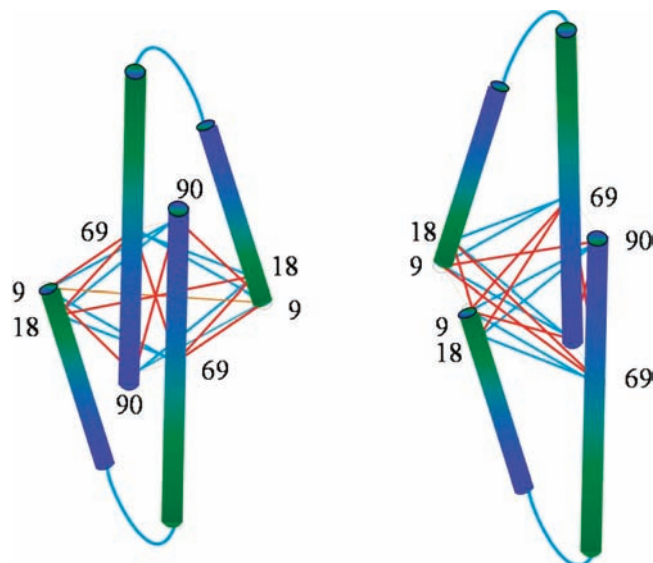

Figure 3. Proposed structures of coexisting dimers A and B of lipid bound αS dimers in agreement with inter- and intramolecular (red and blue lines, respectively) distances measured by DEER; compare Table 1. Interactions between spin labels which could not be detected by DEER are shown as orange lines. The unbound tail (residues 92−140) is not shown.

other. In Table 1, the distances derived from the model are compared to the experimental distances determined, revealing the consistency of these arrangements with the data. Distances below 1.5 and above 4.5 nm will not contribute to the DEER signal under the conditions of the experiment, explaining, for example, that we do not observe the distance of 1.2 nm predicted for dimer B for αS9. Although short distances could, in principle, be detected by line broadening in continuous wave (cw) EPR, simulations show that the combination of a broad distance distribution and the presence of two populations will make detection difficult. It is therefore not surprising that no such broadening could be detected experimentally.

The dimer model presented is the most simple and straightforward interpretation of the data. The dimers could be part of larger aggregates as suggested by AFM,[17] if interactions with additional partners result in spin−spin distances that are larger than the measurement range of the DEER experiment as performed here, i.e. 4.5 nm. Models for small aggregates of αS on membrane surfaces have also been proposed.[16]

The remarkable finding is that the molecules form a well-ordered array upon interacting with the SUVs. Simulation results and experiments support the formation of aggregates on the membrane, without, however, yielding unambiguous experimental evidence for their structure.[16,17,19,31] Our results suggest close association of the helix 2 regions of two αS proteins in an antiparallel arrangement.

At the same time, αS appears to alter the structure of the SUVs. Upon interaction with αS the size of a significant fraction of the SUVs decreases and αS appears to be bound also to such smaller vesicles (see Supporting Information).[17,27] The degree to which the vesicle structure is altered depends on the membrane charge and the size of the vesicles. The strongest effects are seen for the smallest vesicles, made up of purely negatively charged lipids. Increasing the vesicle size or reducing the negative charge density diminishes the effect considerably. The

importance of vesicle size may be related to the presence of membrane curvature stress in the SUVs, which could make it more susceptible for disruption than the membrane in larger vesicles. These results suggest that, under the conditions of the experiment, in the final stage, αS is bound to smaller vesicles or vesicle fragments, rather than to the surface of intact SUVs, as previously assumed.[20] The length scales of such structures may be particularly relevant in the context of the reported interactions of αS with synaptic vesicles.[3]

The intramolecular distance constraints[20] favor the horseshoe conformation. The intermolecular constraints obtained under the same conditions in the present study reveal a close interaction between different αS molecules, which could also explain the horseshoe conformation itself: In dimers, such as the dimer model A, the partner fills the space between helix 1 and 2, providing interactions that may stabilize the horseshoe. This also casts a new light on the ongoing debate[12,20,27,28,30,32−36] of whether αS is in a horseshoe or extended conformation. Obviously, detailed conditions play an important role, and the influence of the details of membrane composition, protein preparation, and vesicle size needs to be carefully controlled and compared.

The results presented here reveal that αS forms well-defined aggregates with lipids. In these aggregates, two αS molecules are in close contact, but they could form part of a larger aggregate in which the proteins are arranged in an ordered fashion. These aggregates could provide nucleation sites that facilitate fibrillization or help sequester αS in a harmless, membrane bound complex. Structural information about the earliest steps of aggregation, as presented here, is the first step toward understanding these mechanisms.

Supporting Information Available: Detailed description of experimental procedure, additional experimental data including Dynamic Light Scattering, Size Exclusion Chromatography using dye-labeled lipids, and vesicle leakage assays, as well as details of the EPR data analysis. This material is available free of charge via the Internet at http://pubs.acs.org.

References

(1) Spillantini, M. G.; Schmidt, M. L.; Lee, V. M. Y.; Trojanowski, J. Q.; Jakes, R.; Goedert, M. *Nature* **1997**, *388* (6645), 839–840.
(2) Goedert, M. *Nat. Rev. Neurosci.* **2001**, *2* (7), 492–501.
(3) Beyer, K. *Cell Biochem. Biophys.* **2007**, *47* (2), 285–299.
(4) Cabin, D. E.; Shimazu, K.; Murphy, D.; Cole, N. B.; Gottschalk, W.; McIlwain, K. L.; Orrison, B.; Chen, A.; Ellis, C. E.; Paylor, R.; Lu, B.; Nussbaum, R. L. *J. Neurosci.* **2002**, *22* (20), 8797–8807.
(5) George, J. M.; Jin, H.; Woods, W. S.; Clayton, D. F. *Neuron* **1995**, *15* (2), 361–372.
(6) Weinreb, P. H.; Zhen, W. G.; Poon, A. W.; Conway, K. A.; Lansbury, P. T. *Biochemistry* **1996**, *35* (43), 13709–13715.
(7) Davidson, W. S.; Jonas, A.; Clayton, D. F.; George, J. M. *J. Biol. Chem.* **1998**, *273* (16), 9443–9449.
(8) Perrin, R. J.; Woods, W. S.; Clayton, D. F.; George, J. M. *J. Biol. Chem.* **2000**, *275* (44), 34393–34398.
(9) Lee, J. C.; Gray, H. B.; Langen, R.; Winkler, J. R. *Biophys. J.* **2004**, *86* (1), 268A.
(10) Ferreon, A. C. M.; Deniz, A. A. *Biochemistry* **2007**, *46* (15), 4499–4509.
(11) Ramakrishnan, M.; Jensen, P. H.; Marsh, D. *Biochemistry* **2003**, *42* (44), 12919–12926.
(12) Jao, C. C.; Der-Sarkissian, A.; Chen, J.; Langen, R. *Biophys. J.* **2004**, *86* (1), 372A.
(13) Ulmer, T. S.; Bax, A.; Cole, N. B.; Nussbaum, R. L. *J. Biol. Chem.* **2005**, *280* (10), 9595–9603.
(14) Lee, H. J.; Choi, C.; Lee, S. J. *J. Biol. Chem.* **2002**, *277* (1), 671–678.
(15) Pandey, A. P.; Haque, F.; Rochet, J. C.; Hovis, J. S. *Biophys. J.* **2009**, *96* (2), 540–551.
(16) Tsigelny, I. F.; Bar-On, P.; Sharikov, Y.; Crews, L.; Hashimoto, M.; Miller, M. A.; Keller, S. H.; Platoshyn, O.; Yuan, J. X. J.; Masliah, E. *FEBS J.* **2007**, *274* (7), 1862–1877.
(17) Jo, E. J.; McLaurin, J.; Yip, C. M.; St George-Hyslop, P.; Fraser, P. E. *J. Biol. Chem.* **2000**, *275* (44), 34328–34334.
(18) Zhu, M.; Fink, A. L. *J. Biol. Chem.* **2003**, *278* (19), 16873–16877.
(19) Ding, T. T.; Lee, S. J.; Rochet, J. C.; Lansbury, P. T. *Biochemistry* **2002**, *41* (32), 10209–10217.
(20) Drescher, M.; Veldhuis, G.; van Rooijen, B. D.; Milikisyants, S.; Subramaniam, V.; Huber, M. *J. Am. Chem. Soc.* **2008**, *130* (25), 7796–7797.
(21) Milov, A. D.; Maryasov, A. G.; Tsvetkov, Y. D. *Appl. Magn. Reson.* **1998**, *15* (1), 107–143.
(22) Jeschke, G.; Polyhach, Y. *Phys. Chem. Chem. Phys.* **2007**, *9* (16), 1895–1910.
(23) Jeschke, G.; Koch, A.; Jonas, U.; Godt, A. *J. Magn. Reson.* **2002**, *155* (1), 72–82.
(24) Schiemann, O.; Prisner, T. F. *Q. Rev. Biophys.* **2007**, *40* (1), 1–53.
(25) Larsen, R. G.; Singel, D. J. *J. Chem. Phys.* **1993**, *98* (7), 5134–5146.
(26) Volles, M. J.; Lee, S. J.; Rochet, J. C.; Shtilerman, M. D.; Ding, T. T.; Kessler, J. C.; Lansbury, P. T. *Biochemistry* **2001**, *40* (26), 7812–7819.
(27) Jao, C. C.; Hegde, B. G.; Chen, J.; Haworth, I. S.; Langen, R. *Proc. Natl. Acad. Sci. U.S.A.* **2008**, *105* (50), 19666–19671.
(28) Georgieva, E. R.; Ramlall, T. F.; Borbat, P. P.; Freed, J. H.; Eliezer, D. *J. Am. Chem. Soc.* **2008**, *130* (39), 12856–12857.
(29) Borbat, P.; Ramlall, T. F.; Freed, J. H.; Eliezer, D. *J. Am. Chem. Soc.* **2006**, *128* (31), 10004–10005.
(30) Chandra, S.; Chen, X. C.; Rizo, J.; Jahn, R.; Sudhof, T. C. *J. Biol. Chem.* **2003**, *278* (17), 15313–15318.
(31) Pandey, A. P.; Haque, F.; Rochet, J. C.; Hovis, J. S. *Biophys. J.* **2009**, *96* (2), 540–551.
(32) Bortolus, M.; Tombolato, F.; Tessari, I.; Bisaglia, M.; Mammi, S.; Bubacco, L.; Ferrarini, A.; Maniero, A. L. *J. Am. Chem. Soc.* **2008**, *130* (21), 6690–6691.
(33) Bussell, R., Jr.; Eliezer, D. *J. Mol. Biol.* **2003**, *329* (4), 763–778.
(34) Bisaglia, M.; Tessari, I.; Pinato, L.; Bellanda, M.; Giraudo, S.; Fasano, M.; Bergantino, E.; Bubacco, L.; Mammi, S. *Biochemistry* **2005**, *44* (1), 329–339.
(35) Bussell, R., Jr.; Ramlall, T. F.; Eliezer, D. *Protein Sci.* **2005**, *14* (4), 862–872.
(36) Trexler, A.; Rhoades, E. *Biochemistry* **2009**, *48*, 2304–2306.

JA909247J